Applied Energy 264 (2020) 114703

Contents lists available at ScienceDirect

Applied Energy

journal homepage: www.elsevier.com/locate/apenergy

2-Amino-2-methyl-1-propanol based non-aqueous absorbent for energy-efficient and non-corrosive carbon dioxide capture

Lv Bihong, Yang Kexuan, Zhou Xiaobin, Zhou Zuoming, Jing Guohua*

College of Chemical Engineering, Huaqiao University, Xiamen 361021, China

HIGHLIGHTS

- 2-amino-2-methyl-1-propanol-based non-aqueous absorbent was used for CO_2 capture.
- Almost 90% of the CO_2 capacity was retained even after 4 regeneration cycles.
- The proposed solution showed non-corrosive behavior after saturated absorption.
- The total heat duty of the solution was half that of a monoethanolamine solution.

GRAPHIC ABSTRACT

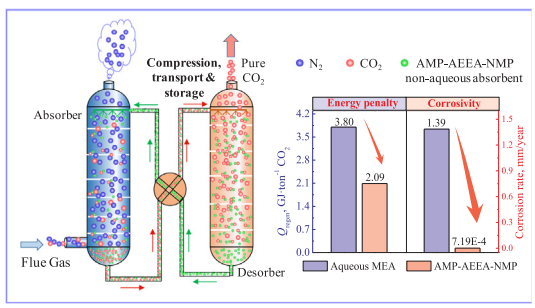

ARTICLE INFO

Keywords:
CO_2 capture
2-Amino-2-methyl-1-propanol
Non-aqueous
Energy conservation

ABSTRACT

The large-scale deployment of carbon dioxide (CO_2) capture using aqueous amines is mainly limited by its intensive energy penalty. In this regard, non-aqueous amine solutions have high energy-saving potential because organics have lower heat capacity and vaporization enthalpy than water. In this study, 2-amino-2-methyl-1-propanol (AMP) coupled with activators in an inert organic solvent (N-methyl pyrrolidone, NMP) is proposed for energy-efficient CO_2 capture. The relationships between activator properties and CO_2 capture performance, such as absorption capacity, regeneration efficiency, and corrosion behavior, were investigated. The results showed that the non-aqueous AMP-AEEA (2-(2-aminoethylamino)ethanol)-NMP solution not only possessed high CO_2 capacity (1.65 mol·kg^{-1} solution) but also retained nearly 90% of its initial CO_2 capacity after the 4th cycle of regeneration. Moreover, it presented a non-corrosive behavior after saturated absorption, clearly showing its superiority over the benchmark monoethanolamine (MEA) solution. The ^{13}C nuclear magnetic resonance (NMR) spectra provided evidence of CO_2 reacting with AMP-AEEA in NMP to form carbamates, which could be easily regenerated under thermal desorption. The specific solvent loss was 0.14 kg·kg^{-1} CO_2 and the total heat duty of AMP-AEEA-NMP solution was only about half that of the MEA solution, which can be attributed to the absence of water and properties of the inert organic solvent. With the perfect CO_2 capture performance, non-corrosive behavior, and significant reduction of energy consumption, the novel solution is a promising candidate for CO_2 capture.

1. Introduction

Carbon dioxide (CO_2) emission from the electricity generating industry significantly contributes to global climate change, which seriously affects global societies and economies [1]. In the short term, carbon capture, utilization and storage (CCUS) is currently considered

* Corresponding author at: Department of Environmental Science & Engineering, Huaqiao University, Xiamen, Fujian 361021, China.
E-mail address: zhoujing@hqu.edu.cn (J. Guohua).

https://doi.org/10.1016/j.apenergy.2020.114703
Received 11 December 2019; Received in revised form 24 January 2020; Accepted 17 February 2020
Available online 05 March 2020
0306-2619/

to be one of the most efficient strategies for mitigating CO_2 emissions [2]. Chemical absorption using organic amine solvents is considered the most mature technology with high selectivity and absorption capacity [3], but with disadvantages of high energy consumption [4] and high corrosiveness [5]. For example, monoethanolamine (MEA)-based aqueous process as an efficient absorbent can increase the cost of electricity (COE) by approximately 80% [6]. Its regeneration heat consumption (about 3.7 GJ/ton CO_2) accounts for more than 60% of COE, which is a major drawback limiting its deployment on a global scale [7]. Thus, the development of advanced absorbents for energy-efficient CO_2 capture has become an urgent demand.

The energy consumption related to solvent regeneration mainly attributed to three factors: (1) the desorption reaction heat (Q_{des}) required to destroy chemical bonds between CO_2 and amines; (2) the sensible heat (Q_{sen}) required to heat the solvent from absorption temperature to regeneration temperature; and (3) the latent heat (Q_{latent}) taken by solvent vapor [8]. For aqueous MEA, due to the large specific heat capacity and vaporization enthalpy of water, the high Q_{sen} and Q_{latent} derived from the heating and vaporization of water incur high energy consumption [9]. Given this, developing energy-efficient absorbents with low Q_{sen} and Q_{sen} is the practical pathway to achieve the ultimate goal of reducing regeneration energy consumption [10]. Some energy efficient absorbents, e.g., biphasic solvents [11], water-lean/free solvents and solvent-free absorbents [12] have shown promising prospect at reducing regeneration heat. Nevertheless, these novel processes are still in the early stages of development, mainly due to the high viscosity of the loaded absorbent and insufficient regeneration efficiency.

Non-aqueous absorbents, consisting of amines and organics such as alcohols [13], ethers [14] and glycols [15], have recently attracted increasing attention owing to their high energy saving potential, low corrosiveness, and low degradation [16], which are promising to be used as cost-effective absorbents for CO_2 capture. Blends of monoethanolamine (MEA) or diethanolamine (DEA) with glycol ethers (2-methoxyethanol (2ME) and 2-ethoxyethanol (2EE)) as nonaqueous solvents could significantly reduce the energy consumption by about 55% as compared to the benchmark aqueous 5.0 mol·L^{-1} (M) MEA system. But the viscosity of MEA/2ME and MEA/2EE increased from 2.6194 mPa·s to 13.717 mPa·s, 3.1120 mPa·s to 22.450 mPa·s after CO_2 absorption [17]. The binary absorbents of conventional amines (MEA and methyldiethanolamine) and ionic liquids had been reported to yield high cycling CO_2 capacity, energy saving, and good regenerability. But the viscosity of MDEA + [BMIM]BF_4 increased from 49.46 mPa·s to 63.40 mPa·s while that of MDEA + [BEIM]BF_4 increased from 49.79 mPa·s to 77.77 mPa·s after saturation with CO_2, and the cycling capacity of MDEA + [BEIM]BF_4 after 3th cyclic number at 358 K was only 84.6% of CO_2 loading for the fresh absorbent [18]. It was found that using N-methylformamide (NMF) greatly enhanced the CO_2 absorption kinetics of MEA, but bad desorption performances and the formation of crystals on the wall of the reactor limited further use of this solvent [19]. The loading capacities of AMP/ethylene glycol/ethanol and AMP/ethylene glycol/1-propanol were found to be 0.92 and 0.87 mol CO_2/mol amine, respectively, and their desorption temperature ranged 353.15–363.15 K in a cyclohexane-aided desorption device. However, higher volatilization of ethanol and cyclohexane posed a problem for industrial application [20]. The MEA-based non-aqueous solvent formed by 2-piperidineethanol (2-PE) and ethylene glycol (EG) exhibited a high CO_2 capacity of up to 0.97 mol CO_2 per mol amine at 298.15 K and 1.0 atm, and it could be released at low temperature (323.15 K) after N_2 sweeping desorption [21]. Nevertheless, its gas was a mixture of CO_2 and N_2, which is not conducive to CO_2 storage in terms of CO_2-capture and storage (CCS). Overall, high volatility, solvent loss, high viscosity, and low regeneration efficiency without N_2 sweeping desorption, become stumbling blocks in the application and development of amine non-aqueous solutions for CO_2 capture.

It remains a challenge to design a absorption system with not only high absorption capacity and low energy requirement, but also low environmental impact and high thermal stability. In this work, a ternary blended non-aqueous absorbent is proposed for CO_2 capture. For this novel solution, 2-amino-2-methyl-1-propanol (AMP), a sterically hindered primary amine with high CO_2 absorption and regeneration capacity [22], with activators was dissolved into an inert organic solvent (N-methyl pyrrolidone, NMP). AMP is the main absorbent providing the CO_2 loading capacity, the activators function as an absorption accelerator to ensure a high absorption rate, and NMP serves as the solvent reducing the energy consumption, attributable to its low heat capacity and vaporization enthalpy and high chemical stability [23]. The performance and mechanism of CO_2 capture into these non-aqueous energy-efficient absorbents are investigated. The regeneration behavior at 120 °C between non-aqueous and MEA aqueous solution are studied to compare the desorption rate and the relative total heat duty. Aqueous 3.0 mol·kg^{-1} MEA was used a baseline solvent for the comparison. The proposed solvent is expected to provide improved performance, efficient energy consumption, and non-corrosive behavior.

2. Materials and methods

2.1. Chemicals

2-Amino-2-methyl-1-propanol (AMP, 98%), monoethanolamine (MEA, 99%), 2-(2-aminoethylamino)ethanol (AEEA, 98%), 3-(methylamino)propylamine (MAPA, 99%), diethylenetriamine (DETA, 99%), piperazine (PZ, 99%), triethylenetetramine (TETA, 70%), and N-methyl pyrrolidone (NMP, 99.5%) were all purchased from Chengdu XiYa Chemical Technology Co., Ltd., China. Deuterochloroform ($CDCl_3$) was supplied by J&K Scientific Ltd. The CO_2 gas (99.99 vol%) was provided by Fujian Nanan Chenggong Gas Co., Ltd., China. A low-cost equipment material in CO_2 capture facilities, 20# carbon steel with a size of 20 mm × 10 mm × 2 mm supplied by Yangzhou Xiangwei Machine Co., Ltd., China), was used in the corrosion experiments. All the chemicals for experiments were used without any further purification. The non-aqueous solution is composed of AMP (2.5 mol·kg^{-1}) and activator (0.5 mol·kg^{-1}) dissolved in the NMP solution, and the total solution was maintained at 0.025 kg.

Six common activators including two alkanolamines (MEA and AEEA) and four alkylamines (PZ, MAPA, DETA, and TETA) were selected as preliminary activators to constitute a novel AMP-activator-NMP non-aqueous absorbent. Table 1 shows the names (abbreviations), chemical structures and the physicochemical properties of these activators.

2.2. CO_2 absorption and desorption

The CO_2 absorption experiment was carried out in a custom-fabricated bubbling reactor, which has been described in our previous work [10]. In a typical test, about 25 g of the non-aqueous solution, in which the concentration of AMP and activator were 2.5 and 0.5 mol·kg^{-1}, respectively, was placed in the reactor and heated to a desired temperature. Afterwards, CO_2 was continuously bubbled into the solution at a flow rate of 80 mL·min^{-1} controlled by a mass flowmeter. The inlet and outlet gas flow rates of the reactor were measured using a soap-film flowmeter under the atmosphere. The CO_2 absorption rate (r_{ab}; mol·min^{-1}·kg^{-1}) was determined based on the difference between the inlet and outlet gas flow rates. The CO_2 absorption capacity (R, mol·kg^{-1}) can be calculated by integrating the absorption rate against the absorption time.

As the absorbent was saturated, the solution was sent to a desorption reactor at 393.15 K under the atmosphere. CO_2 desorption rate was measured using a soap-film flowmeter. When no further changes occurred in the soap film in the flowmeter, the desorption was assumed to be complete. The regeneration ratio (η, %) was determined as a

Table 1
Properties of six common activators.

Activator	Structural formula	Molecular weight	Boiling point (°C)	Vapor pressure (mmHg)
MEA	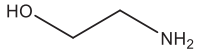	61.08	170	0.2 (20 °C)
PZ	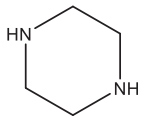	86.14	146	0.8 (20 °C)
MAPA	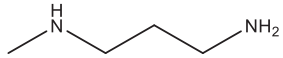	88.15	140	6.3 (25 °C)
AEEA	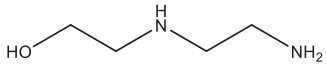	104.15	240	0.031 (25 °C)
DETA	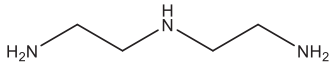	103.17	204	0.08 (20 °C)
TETA	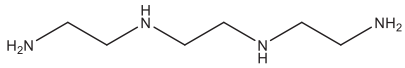	146.23	267	< 0.01 (20 °C)

measure of the ratio between the cyclic capacity (ΔR, mol·kg^{-1}) and the absorption capacity of the absorbent. Equations of these parameters are detailed in Supplementary data.

2.3. Evaluation of regeneration heat duty

The vapor-liquid equilibrium (VLE) data were collected in an air-tight reactor, as shown in Fig. 1. Firstly, N_2 was purged into the reactor to remove residual air (< 5 KPa) and a constant gas phase partial pressure was maintained, after which 200 mL of the non-aqueous solution was poured into the reactor. When equilibrium was reached, a certain amount of CO_2 was supplied to the gasholder and transferred to the reactor to achieve a certain gas partial pressure, and the solvent subsequently reached the vapor-liquid equilibrium. The CO_2 absorption loading of the absorbent was calculated according to the decrease of gas phase pressure. The regeneration heat duty (Q_{regen}, GJ·ton^{-1} CO_2) consists of three parts [24], desorption reaction heat (Q_{des},), sensible heat (Q_{sen}), and latent heat (Q_{latent}) [25], as defined in Eq. (1). The individual energy terms can be expressed by Eq. (2) [26].

$$Q_{regen} = Q_{des} + Q_{sen} + Q_{latent} \tag{1}$$

$$Q_{regen} = \frac{-\Delta H_{abs}}{M} + \frac{C_p \times m_{sol} \times \Delta T}{m_{CO_2}} + \frac{m_{sol}^{vap}}{m_{CO_2}} \Delta H_{sol}^{vap}(T_R) \tag{2}$$

where ΔH_{abs} is the reaction enthalpy of CO_2 absorption, kJ·mol^{-1}; M is the CO_2 molecular weight, 44 g·mol^{-1}; C_p is the heat capacity of the solution, kJ·K^{-1}·kg^{-1}; m_{sol} and m_{CO2} are the masses of the solution for regeneration and the desorbed CO_2, respectively, kg; ΔT is the temperature difference between the rich and lean solutions and is set as 10 K; m_{sol}^{vap} is the amount of solvent loss during regeneration, kg; $\Delta H_{sol}^{vap}(T_R)$ is the vaporization enthalpy of the solution at the regeneration temperature, kJ·kg^{-1}. The parameters required for the calculation of regeneration heat are summarized in the Table S1-3 of the Supporting Information. According to the above equations, the values of Q_{des}, Q_{sen} and Q_{latent} were calculated, as listed in Table S4 of the Supporting Information.

2.4. Corrosivity test

The corrosivity of the novel non-aqueous solution was explored by determining the corrosion behavior of carbon steel in the tested solution. For a typical experiment, fresh or CO_2-saturated solution was prepared and poured into a 50 mL colorimetric tube, wherein a cleaned 20# carbon steel coupon was immersed. The colorimetric tube was placed in the thermostat water bath to ensure a constant temperature (313.15 K). Then, the corrosion status of the coupon was monitored and recorded at a certain time interval. Meanwhile, the corrosion rate of

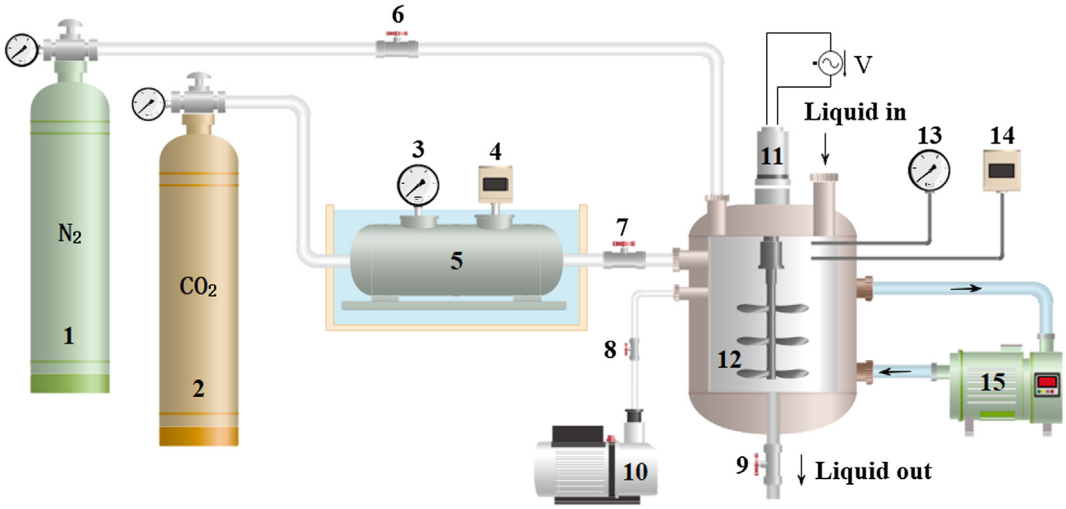

Fig. 1. Schematic diagram of experimental set up for determining VLE data. (1 N_2 cylinder; 2 CO_2 cylinder; 3, 13 pressure gage; 4, 14 thermometer; 5 gasholder; 6, 7, 8, 9 valve; 10 vacuum pump; 11 magnetic-driving system; 12 reactor; 15 thermostat water circulating pump).

carbon steel in the test solution was determined by another electrochemical experiment, which was conducted using an electrochemical workstation. The detailed procedure of the electrochemical experiment is available in our previous work [27].

2.5. ^{13}C NMR analysis

Reaction products formed in the novel non-aqueous system during CO_2 capture were identified by ^{13}C NMR spectra obtained from a Bruker AVIII 500 MHz NMR spectrometer. To prepare a sample for detection, 0.3 mL of the solution was sampled and introduced into the nuclear magnetic resonance tube, using 0.3 mL of CD_3OD as an internal standard for deuterium lock.

3. Results and discussion

3.1. Activator properties-CO_2 capture performance relationship

3.1.1. CO_2 absorption performance

After CO_2 absorption, there were obvious differences in the state of these six different AMP-activator-NMP non-aqueous absorbents, and the photos were shown in Fig. 2. The observation results indicated that after saturated absorption, the AMP- NMP solution activated by MEA, MAPA or AEEA remained in a clear and transparent state without any stratification, flocculation, and demulsification, while powder or gel-like products formed with the introduction of PZ, DETA, and TETA. The latter phenomenon was largely due to the strong hydrogen bonds [28] of the reaction products between CO_2 and PZ, DETA, or TETA. The hydrogen bond length and dipole moment of the products of the reaction of CO_2 with MEA, MAPA, AEEA, PZ, DETA, and TETA into NMP were calculated using the density functional theory (DFT) method in the Gaussian 09 software package. The calculated results are provided in Table S2 in Supporting Information. Although the hydrogen bond lengths of the first three systems were slightly lower than that of the latter ones, there was no obvious difference between them. Meanwhile, the dipole moment values of the products of the first three systems into NMP were found to be all much higher than those of the latter ones, which implies higher viscosity and resulted in the stratification, flocculation, and demulsification. Such solid-like products would cause clogging of the absorber, which is disadvantageous to the absorption and actual operation. Thus, PZ, DETA, and TETA were all excluded from the screening as they are not suitable as activators for the AMP-NMP solution. The remaining activators (MEA, MAPA, and AEEA) were considered for further analysis.

Based on the above pre-screening test, CO_2 absorption into three non-aqueous systems, i.e., AMP-MEA-NMP, AMP-MAPA-NMP, and AMP-AEEA-NMP, was further carried out to determine the most effective activator. In addition, the performances of non-aqueous AMP-NMP and aqueous MEA solutions were evaluated as comparison groups. For all solutions, the total amine concentration was kept at 3.0 mol·kg^{-1}. CO_2 absorption performances of some different absorbents are presented in Fig. 3. At the initial period of the investigation, CO_2 was completely absorbed into the solvents into the bubbling absorber due to a high concentration of the absorbent, and it was difficult to identify the effects of activators on the CO_2 absorption rate and capacity of the solutions. As the reaction proceeded, the absorption rates of these solutions decreased, while their capacities increased and then tended towards stability until the solutions were saturated. The solutions containing activators took longer to reach saturation than the AMP-NMP solution, indicating an intensifying effect of the activators. The CO_2 capacity of the AMP-NMP solution was found to be 1.16 mol·kg^{-1}, which was much less than that of the MEA (1.80 mol·kg^{-1}) and AMP-H_2O (2.68 mol·kg^{-1}) solutions. The CO_2 capacity increased to different degrees when a fraction of AMP was substituted by the activators. in particular, the CO_2 capacities of the AMP-MAPA-NMP and AMP-AEEA-NMP systems were 1.60 and 1.65 mol·kg^{-1}, respectively, which were close to that of the MEA aqueous solution. As a tertiary amine, the reaction between AMP and CO_2 almost follow an equal mole reaction but at a slow rate. In the non-aqueous solution, the reaction product of AMP with CO_2 cannot undergo hydrolysis and the viscosity of the solution increases, resulting in a lower absorption capacity of the system. With the promotion of the

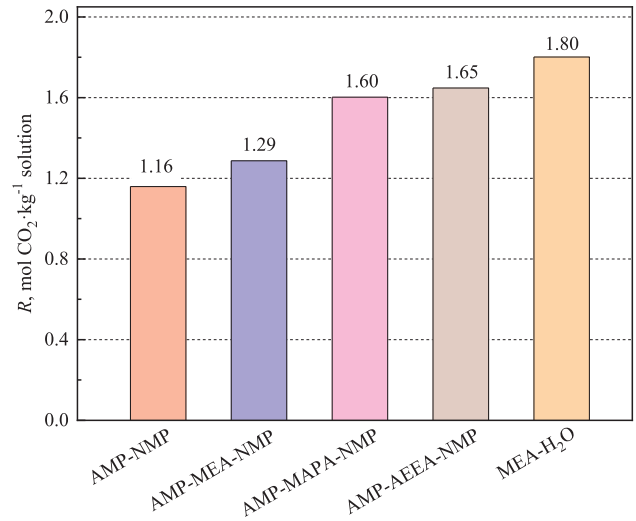

Fig. 3. CO_2 absorption capacity of different absorbents. (C_{total}: 3.0 mol·kg^{-1}; Q_{CO2}: 80 mL·min^{-1}; V_L: 25 g; $T_{absorption}$: 313.15 K).

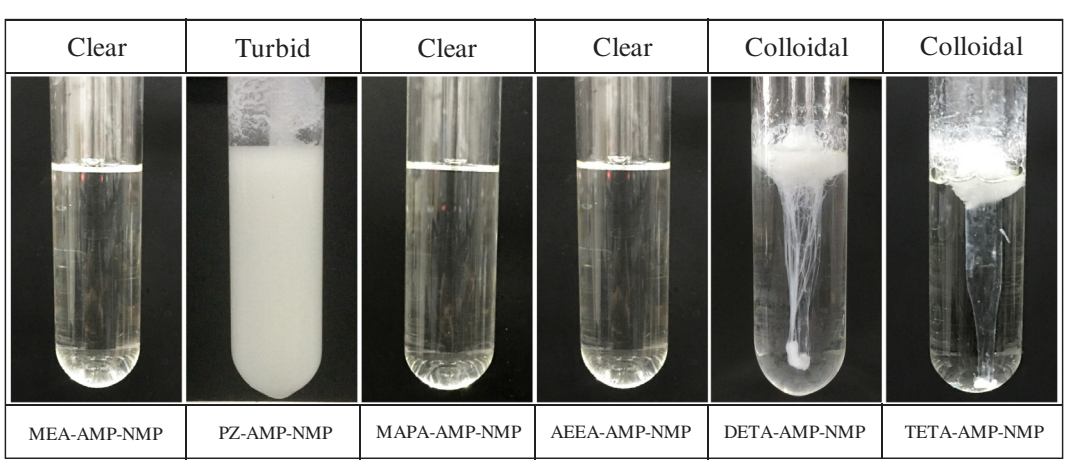

Fig. 2. Photos of different solutions after CO_2 bubbling. (C_{AMP}: 2.5 mol·kg^{-1}; $C_{activator}$: 0.5 mol·kg^{-1}; V_L: 25 g; $T_{absorption}$: 313.15 K).

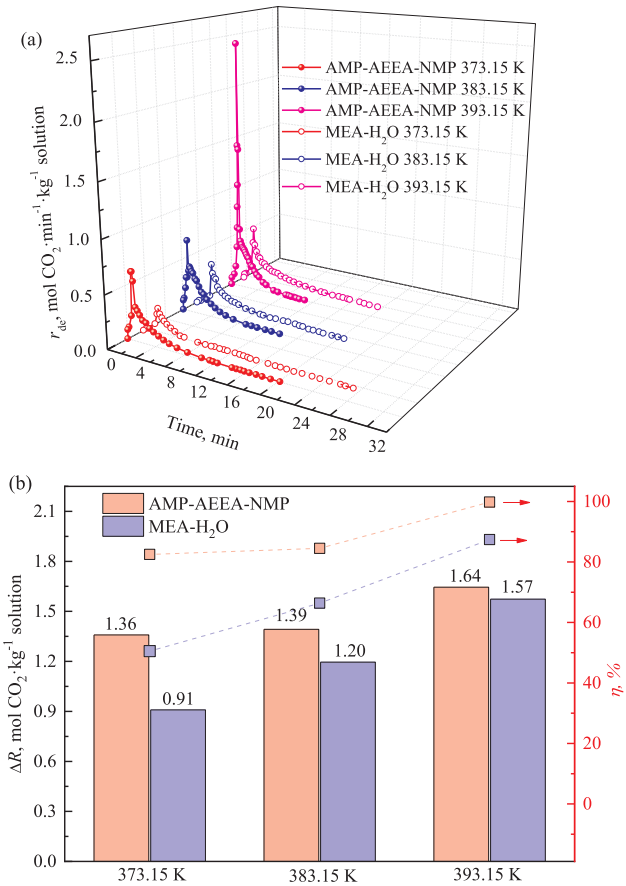

Fig. 4. CO_2 desorption from CO_2-loaded solutions at different temperature: (a) desorption rate, (b) cyclic capacity and regeneration efficiency (C_{AMP}: 2.5 mol·kg^{-1}; C_{AEEA}: 0.5 mol·kg^{-1}; C_{MEA}: 3.0 mol·kg^{-1}; V_L: 25 g; $T_{absorption}$: 313.15 K).

activators, the absorption rate and capacity of the solutions were increased.

According to the above results, it could be concluded that introducing an activator into the AMP-NMP non-aqueous solution was beneficial in terms of the improvement of both the CO_2 absorption rate and CO_2 capacity. Basically, MAPA and AEEA exhibited equivalent activation effects on promoting the CO_2 absorption performance. Nevertheless, AEEA possesses superior properties (e.g., high boiling point and low vapor pressure) than MAPA (as presented in Table 1). Accordingly, AEEA was considered the optimal activator for the AMP-NMP non-aqueous solution. Therefore, the AMP-AEEA-NMP non-aqueous solution was further analyzed.

3.1.2. CO_2 desorption performance

Desorption performance is another important parameter for evaluating an absorbent. In the present work, the desorption performance of the AMP-AEEA-NMP solution was investigated in terms of CO_2 desorption rate, cyclic capacity and regeneration ratio at a temperature range of 373.15–393.15 K in an oil bath. The MEA-H_2O solution was also investigated for comparison. The results are depicted in Fig. 4.

Fig. 4(a) displays the change in the CO_2 desorption rate of the AMP-AEEA-NMP and MEA-H_2O solutions versus time at different desorption temperatures. The desorption rates of all solutions increased at the initial stage (0–1.5 min) as the solutions were rapidly heated to the desired regeneration temperature from the absorption temperature (313.15 K). After the CO_2 desorption rates reached their maximum, they gradually decreased as the absorbed CO_2 was continuously released from the solution. In contrast, the maximum desorption rates of AMP-AEEA-NMP were higher than those of MEA-H_2O at the same regeneration temperature. In particular, the former could reach as high as 2.43 mol CO_2·min^{-1}·kg^{-1} at 393.15 K, which was 4.4 times higher than that of MEA-H_2O. On the other hand, regardless of the regeneration temperature, the completion time of CO_2 desorption for AMP-AEEA-NMP was shorter than that for MEA-H_2O. Due to the steric effect, the carbamates formed by the reaction between AMP and CO_2 were more unstable than those by the MEA solution, which can regenerate easily to improve the regeneration rate and efficiency during thermal desorption [29]. Thus, the AMP-AEEA-NMP blends reached the highest desorption rate in comparison with the MEA based absorbent. Fig. 4(b) shows that the CO_2 cyclic capacities (ΔR) and the regeneration efficiencies (η%) of the AMP-AEEA-NMP solution were higher than those of the MEA-H_2O solution at the same regeneration temperature, although they all increased with increasing regeneration temperature. The regeneration efficiency of the non-aqueous solution was up to 99.4% while that of MEA was only 87.2%. Fast desorption rate, higher regeneration efficiency, and shorter desorption time favor the shortening of the desorption time or volume of the desorption column, resulting in lower cost and higher profits.

To verify the stability of the AMP-AEEA-NMP system, the CO_2-saturated solution was regenerated by thermal desorption, and subsequently reused to absorb CO_2. The absorption–desorption cycle experiments were performed four times, and the results are shown in Fig. 5. It should be noted that no additional solvent was added during the tests to compensate for the solvent loss caused by evaporation. The CO_2 absorption capacity of the AMP-AEEA-NMP solution was found to slightly decrease with increasing iterations of the absorption–desorption cycle, but it still reached 1.48 mol CO_2·kg^{-1} solution and retained nearly 90% of its initial CO_2 capacity even after the 4th cycle. The results indicate that the CO_2 capture process by AMP-AEEA-NMP is fairly reversible and easy to operate.

3.1.3. Corrosivity of the non-aqueous absorbent

As equipment corrosion is one of the main challenges in CO_2 capture with chemical absorbents, the behavior of the solvent becomes an important criterion in absorbent screening [30]. To investigate the corrosion behavior, 20# carbon steel were immersed in CO_2-saturated solutions and checked regularly to observe any changes in the solution and carbon steel. The observation was started the moment the carbon steel was immersed into the solution, and this moment was defined as Day 0. An obvious change in color of the solutions was observed. The solutions became darker and turbidity increased with increasing immersion time, indicating that the extent of corrosion was aggravated

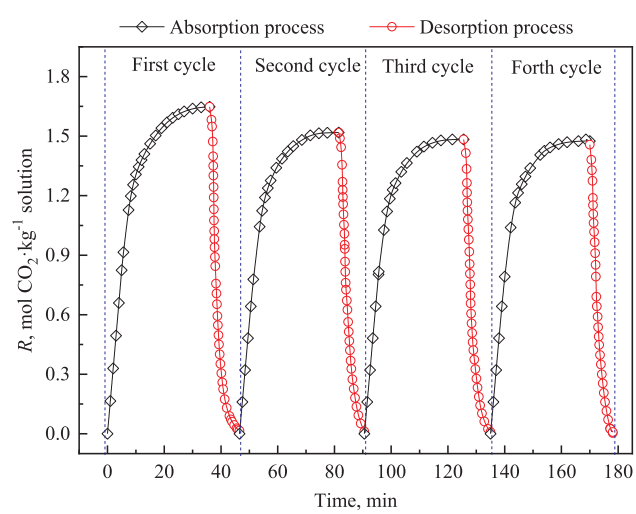

Fig. 5. CO_2 absorption–desorption cycles of AMP-AEEA-NMP solution. (C_{AMP}: 2.5 mol·kg^{-1}; C_{AEEA}: 0.5 mol·kg^{-1}; V_L: 25 g; $T_{absorption}$: 313.15 K, $T_{desorption}$: 393.15 K).

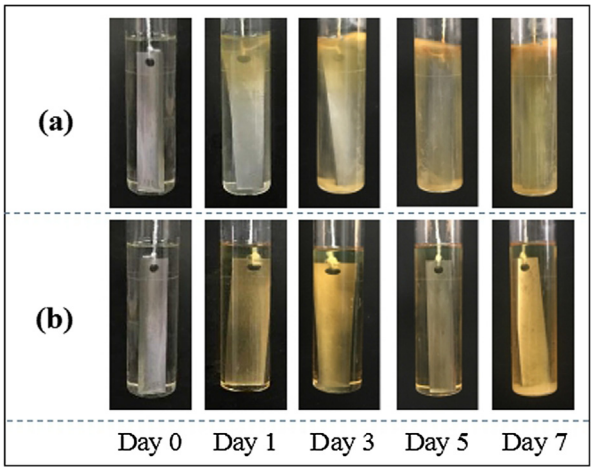

Fig. 6. Photos of CO_2-saturated solutions during corrosion test. (a) aqueous MEA solution; (b) non-aqueous AMP-AEEA-NMP solution. (C_{AMP}: 2.5 mol·kg^{-1}; C_{AEEA}: 0.5 mol·kg^{-1}; C_{MEA}: 3.0 mol·kg^{-1}; V_L: 25 g; T: 313.15 K).

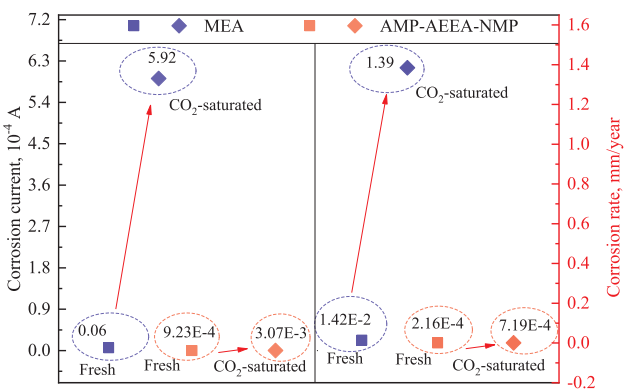

Fig. 7. Corrosion behavior of 20# carbon steel coupons in aqueous MEA and non-aqueous AMP-AEEA-NMP solutions (left side: corrosion current; right side: corrosion rate) (C_{AMP}: 2.5 mol·kg^{-1}; C_{AEEA}: 0.5 mol·kg^{-1}; C_{MEA}: 3.0 mol·kg^{-1}; V_L: 25 g; T: 313.15 K).

(Fig. 6). However, the AMP-AEEA-NMP saturated solutions became darker after long-term installation even without the immersion of the carbon steel. Therefore, the color of the solution may not directly correspond to the corrosion level. Moreover, the color of AMP-AEEA-NMP appeared to be darker than that of the MEA saturated solution at the same immersion time, which could be confusing and even counterproductive. Thus, the corrosion behavior of different solutions, e.g., the corrosion current and corrosion rate, were measured through further electrochemical experiment. Fig. 7 shows the results of the corrosion test, with corrosion current on the left column and corrosion rate on the right. The corrosion current and corrosion rate of fresh AMP-AEEA-NMP and MEA solutions were both extremely low, indicating low-corrosiveness of the fresh solution. In the saturated solution, some obvious differences were observed between the two solutions. The corrosion current and corrosion rate of the CO_2 saturated MEA were significantly enhanced, indicating its strong corrosion behavior. In contrast, the corrosion current and corrosion rate of AMP-AEEA-NMP were only slightly increased after saturated absorption and were much lower than those of MEA. On the one hand, it has been proved that AMP based solutions can preferentially produce surface $FeCO_3$ layers to provide sufficient protection from continued corrosion of the carbon steel, while there was no siderite layer of the carbon steel in the saturated MEA solution in the reported work [31]. On the other hand, the carbamates of MEA could easily hydrolyze into HCO_3^-/CO_3^{2-} in aqueous solutions but not in non-aqueous solutions, and the dissociation of CO_2 products would increase oxidizing substances in the solution, which further enhances the corrosion of carbon steel. Thus, the corrosivity of the non-aqueous system is lower than that of traditional aqueous MEA solutions. Nevertheless, their corrosion rates were all below 0.1 mm/year [27], indicating a non-corrosive CO_2 capture of the AMP-AEEA-NMP, which is conducive to industrial production and application.

3.2. CO_2 capture mechanism

3.2.1. ^{13}C NMR spectra of the CO_2 absorption-desorption process

The molecular structures of products in the solutions during the CO_2 capture process were confirmed by ^{13}C NMR, and the results are shown in Fig. 8. Since the solution was soluble in CD_3OD and insoluble in other deuterated reagents, CD_3OD was used as an internal standard for deuterium lock in the test. In the primary amine aqueous solution, two new signals appeared at 165.3 and 160.2 ppm in the CO_2 loaded solution, which were attributed to carbamate and bicarbonate/carbonate species, respectively. At high CO_2 loading, carbamates might hydrolyze to form protonated amine and bicarbonate [32]. Due to the absence of water (Fig. 8a), there were only new peaks at 164.0 ppm as the CO_2 loading of the solution increased from 0 to 0.49 mol kg^{-1}. At this time, the primary amine of AMP and AEEA could react with CO_2, forming unstable carbamates [33]. As the CO_2 loading further increased, the intensity of the carbamates signals increased, and a new alkyl carbonate signal appeared at 159.3 ppm. In the saturated solution, the carbamate signal still existed but its intensity was slightly reduced, while the intensity of carbonate was obviously increased. In order to clarify the interaction between the absorbents and CO_2, a comparative experiment was carried out. CO_2 was continuously supplied to the AMP-NMP solution until it was saturated. Subsequently, AEEA was added to the saturated AMP-NMP solution, in which their concentrations were the same as those of AMP-AEEA-NMP in Fig. 8a. As shown in Fig. 8b, the signals of carbamates and alkyl carbonate all appeared in the saturated AMP-NMP, and the signal intensity of carbamates increased while that of carbonate decreased when AEEA was added. The results indicate that these two products interconvert into each other during the absorption. During the desorption process (Fig. 8c), the signals were found to be in the opposite direction to those of the absorption process. The signals of carbamates decreased under thermal desorption, while carbonates disappeared rapidly and a weak signal of carbamates was observed in the final solution, suggesting incomplete desorption.

3.2.2. Mechanism of CO_2 capture into AMP-AEEA-NMP

Based on the results of the capture performance and ^{13}C NMR spectra, the mechanisms of CO_2 capture in AMP-AEEA-NMP were clarified. During the absorption, CO_2 first reacted with the primary amine of AMP and AEEA (R-NH2) to form unstable carbamates, and the reaction equations are expressed as follows:

$$R\text{-}NH_2 + CO_2 \leftrightarrow RNHCOOH \tag{3}$$

$$2R\text{-}NH_2 + CO_2 \leftrightarrow R\text{-}NHCOO^- + R\text{-}NH_3^+ \tag{4}$$

It has been proven that carbamates easily hydrolyze in aqueous solutions with H_2O and form carbonates during the absorption [34]. In the present work, NMP was used to replace water, and hydrolysis reactions were prevented because NMP chemically stable and inert to CO_2 absorption [35]. Nevertheless, the ^{13}C NMR spectra showed that carbonates were produced in the late stage of absorption, which is not attributable to the hydrolysis of NMP. As mentioned above, CD_3OD was added as an internal standard for deuterium lock to the mixture of AMP-AEEA-NMP. In our previous work, the carbamate product of AMP was found to be unstable in the presence of ethanol and would decompose into carbonates. Thus, the carbonates in the AMP-AEEA-NMP are attributable to the hydrolysis of carbamates by CD_3OD.

As base species in the mixture, AMP and AEEA can also react with the carbamate products. The reaction can be expressed as:

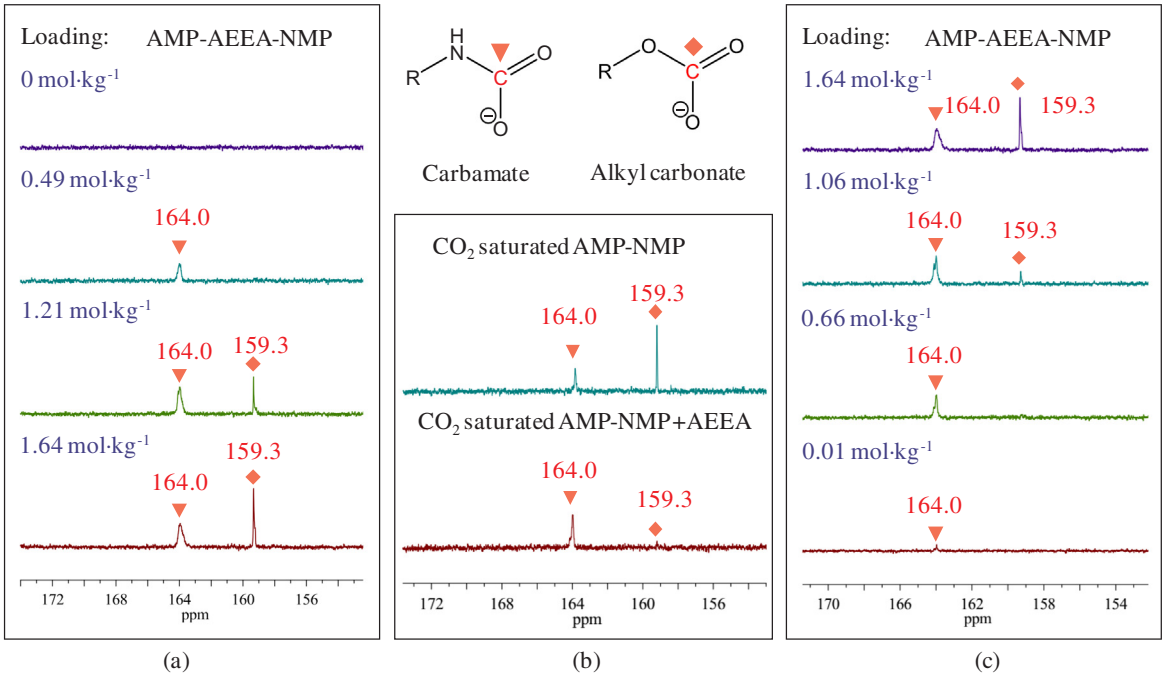

Fig. 8. ^{13}C NMR spectra of AMP-AEEA-NMP during CO_2 capture process. (a) and (b) absorption (c) desorption. (C_{AMP}: 2.5 mol·kg^{-1}; C_{AEEA}: 0.5 mol·kg^{-1}).

$$R1\text{-}NHCOO^- + R2\text{-}NH_2 \leftrightarrow R1\text{-}NH_2 + R2\text{-}NHCOO^- \quad (5)$$

During the desorption process, the carbamates are regenerated under thermal desorption, and CO_2 is continuously released from the loaded solution, which is an inverse process of absorption.

3.3. Thermodynamics of CO_2 capture into AMP-AEEA-NMP

3.3.1. Solvent vaporization loss

The specific solvent loss of MEA and AMP-AEEA-NMP at different desorption temperatures were compared, as shown in Fig. 9. The results showed that the specific solvent loss of MEA decreased and that of AMP-AEEA-NMP slightly increased with increasing regeneration temperatures. Since the specific solvent loss is defined as the accompanying solvent loss per unit mole of removed CO_2 [36], its value is obviously affected by the CO_2 cyclic capacity. On one hand, higher regeneration temperatures increase the CO_2 cyclic capacity, while on the other hand, it also increases solvent loss due to vaporization. As mentioned in Fig. 4b, the CO_2 cyclic capacities (ΔR) of the AMP-AEEA-NMP and MEA-H_2O solutions both increased as the regeneration temperature increased, and the amount of increase was slightly higher in the former

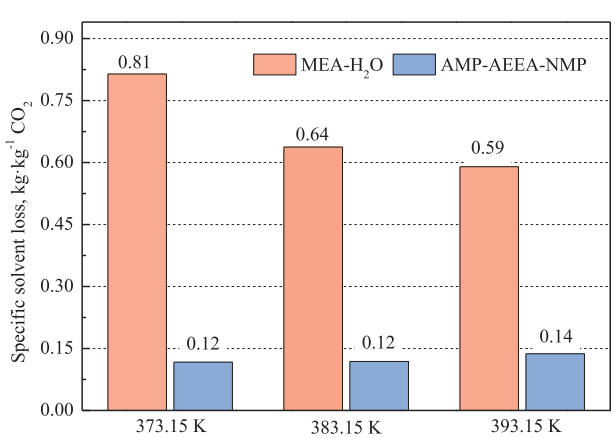

Fig. 9. Specific solvent loss of various absorbents at different regeneration temperatures (C_{AMP}: 2.5 mol·kg^{-1}; C_{AEEA}: 0.5 mol·kg^{-1}).

than in the latter because of unstable carbamates of AMP-CO_2. For the MEA solution, a substantial increase of cyclic capacity led to decreased specific solvent loss with increasing temperature. However, such a promoting effect on CO_2 cyclic capacity is limited in the AMP-AEEA-NMP solution, but the solvent evaporation becomes more apparent. Thus, the specific solvent loss of AMP-AEEA-NMP slightly increased with increasing desorption temperature. However, the specific solvent loss of the AMP-AEEA-NMP solution (0.14 kg·kg^{-1} CO_2) were all much lower than that of the MEA solution under the same condition, which can be attributed to the lower volatility of the inert organic solvent.

3.4. Heat duty of the regeneration process

In light of the good CO_2 absorption and desorption performance, the non-aqueous AMP-AEEA-NMP solution is believed to be an efficient absorbent. To evaluate the potential of the AMP-AEEA-NMP solution as an alternative to conventional aqueous MEA solution, its regeneration heat duty was determined, and the results are shown in Fig. 10. The heat duty of both these two solutions decreased as the desorption temperature increased. The regeneration heat duty (Q_{regen}) for the CO_2-loaded solutions comprised three parameters, and the detailed composition of the energy penalty for each solution was quite different, especially with regard to Q_{sen} and Q_{latent}. Q_{sen} is the energy required to heat the absorbent from the absorption temperature to the regeneration temperature, which is correlated with the heat capacity of the solution [37]. As the heat capacity of the organic solvent (NMP) was much lower than that of H_2O, the Q_{sen} value of the AMP-AEEA-NMP solution was lower than that of the MEA solution. Q_{latent} is the vaporization heat due to solvent vaporization during CO_2 desorption, and depends mainly on the vaporization enthalpy of the solvent [38]. As mentioned above, NMP is an inert organic solvent and chemically stable. Thus, the vaporization enthalpy of NMP was much lower than that of H_2O, resulting a lower value of Q_{latent}. Unlike these two parameters, Q_{des} is considered to equal the heat released from the reaction of the CO_2 product formation. Thus, the Q_{des} values of these two solutions were similar (nearly 1.80 GJ ton^{-1} CO_2) due to their similar carbamate products. As shown in Fig. 4(B), the CO_2 cyclic capacities (ΔR) and regeneration efficiencies (η%) of the AMP-AEEA-NMP and MEA-H_2O solutions both increased with increasing regeneration temperature. Thus, a higher

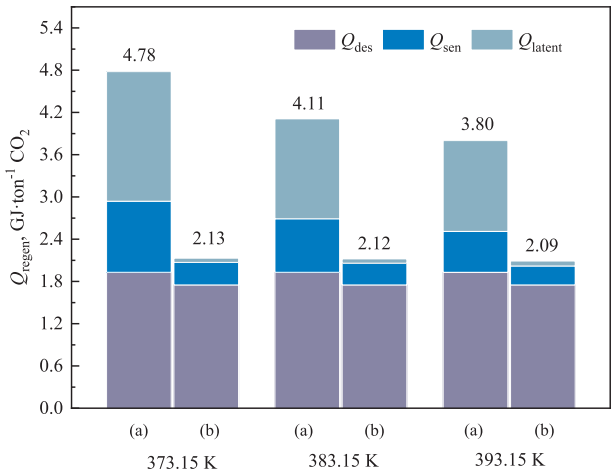

Fig. 10. Energy penalties for absorbents at different regeneration temperatures. (a) MEA solution (b) AMP-AEEA-NMP non-aqueous solution. (C_{AMP}: 2.5 mol·kg^{-1}; C_{AEEA}: 0.5 mol·kg^{-1}; C_{MEA}: 3.0 mol·kg^{-1}; V_L: 25 g; T: 313.15 K).

desorption temperature implies a higher desorption rate, higher regeneration efficiency, and shorter desorption time, which also results in lower energy penalties. On the whole, the total heat duty of the AMP-AEEA-NMP solution was much lower and only about half that of the MEA solution, which further prove its potential as an energy-saving alternative for CO_2 capture.

4. Conclusions

This work proposed a novel non-aqueous solution for CO_2 capture. In the mixture, AMP as the main absorbent ensured high CO_2 capacity, AEEA as the activator accelerated the absorption rate of the solution, and NMP as the solvent provided high chemical stability and favorable physicochemical properties. The CO_2 capacity of the AMP-AEEA-NMP system was 1.65 mol·kg^{-1}. Even with the unstable CO_2 products of carbamates, the solution still achieved a CO_2 capacity of 1.48 mol CO_2·kg^{-1} after the 4th cycle of regeneration, which accounts for a retention of nearly 90% of its initial CO_2 capacity. With the lower heat capacity and vaporization enthalpy of NMP, the total heat duty of the AMP-AEEA-NMP solution was found to be 2.09 GJ ton^{-1} CO_2 at 393.15 K desorption temperature, which was only about half that of the MEA solution. In conclusion, the possible advantages offered by the non-aqueous amines (AMP-AEEA-NMP) over the conventional aqueous technique make it a highly feasible alternative in the field of post-combustion CO_2 capture.

CRediT authorship contribution statement

Lv Bihong: Conceptualization, Methodology, Writing - review & editing. **Yang Kexuan:** Visualization, Investigation, Data curation. **Zhou Xiaobin:** Investigation, Writing - original draft. **Zhou Zuoming:** Supervision, Validation. **Jing Guohua:** Supervision.

Declaration of Competing Interest

The authors declare that they have no known competing financial interests or personal relationships that could have appeared to influence the work reported in this paper.

Acknowledgments

This work was sponsored by the National Natural Science Foundation of China (21876053, 21808074 and 21676110), and the Promotion Program for Young and Middle-aged Teachers in Science and Technology Research of Huaqiao University (ZQN-YX603). We also thank the Instrumental Analysis Center of Huaqiao University for analysis support.

Appendix A. Supplementary data

Supplementary data to this article can be found online at https://doi.org/10.1016/j.apenergy.2020.114703.

References

[1] Solomon SD, Qin D, Manning M. Climate Change 2007: The Physical Science Basis. Working Group I Contribution to the Fourth Assessment Report of the IPCC Intergovernmental Panel on Climate Change Climate Change 2001;18:95–123.
[2] Wang LD, Yu SH, Li QW, Zhang YF, An SL, Zhang SH. Performance of sulfolane/DETA hybrids for CO_2, absorption: phase splitting behavior, kinetics and thermodynamics. Appl Energ 2018;228:568–76.
[3] Jing GH, Qian YH, Zhou XB, Lv BH, Zhou ZM. Designing and screening of multi-amino-functionalized ionic liquid solution for CO_2 capture by quantum chemical simulation. ACS Sustain Chem Eng 2018;6:1182–91.
[4] Zhang SH, Shen Y, Wang LD, Chen JM, Lu Y. Phase change solvents for post-combustion CO_2 capture: principle, advances, and challenges. Appl Energ 2019;239:876–97.
[5] Zhang SH, Du MN, Shao PJ, Wang LD, Ye JX, Chen J, et al. Carbonic anhydrase enzyme-MOFs composite with a superior catalytic performance to promote CO2 absorption into tertiary amine solution. Environ Sci Technol 2018;52:12708–16.
[6] Allam RJ, Palmer MR, Brown GW, Fetvedt J, Freed D, Nomoto H, et al. High efficiency and low cost of electricity generation from fossil fuels while eliminating atmospheric emissions, including carbon dioxide. Energ Procedia 2013;37:1135–49.
[7] Zhang XW, Zhu ZQ, Sun XY, Yang J, Gao HX, Huang YQ, et al. Reducing energy penalty of CO_2 capture using Fe promoted SO_4^2/ZrO_2/MCM-41 catalyst. Environ Sci Technol 2019;53:6094–102.
[8] Zhang SH, Shen Y, Shao PJ, Chen JM, Wang LD. Kinetics, thermodynamics, and mechanism of a novel biphasic solvent for CO_2 capture from flue gas. Environ Sci Technol 2018;52:3660–8.
[9] Maneeintr K, Idem RO, Tontiwachwuthikul P, Wee AGH. Comparative mass transfer performance studies of CO_2 absorption into aqueous solutions of DEAB and MEA. Ind Eng Chem Res 2010;49:2857–63.
[10] Zhou XB, Jing GH, Lv BH, Liu F, Zhou ZM. Low-viscosity and efficient regeneration of CO_2 capture using a biphasic solvent regulated by 2-amino-2-methyl-1-propanol. Appl Energ 2019;235:379–90.
[11] Wang LD, Zhang YF, Wang RJ, Li QW, Zhang SH, Li M, et al. Advanced monoethanolamine absorption using sulfolane as a phase splitter for CO_2 capture. Environ Sci Technol 2018;52:14556–63.
[12] Guo H, Li H, Shen SF. CO_2 capture by water-lean amino acid salts: absorption performance and mechanism. Energ Fuel 2018;32:6943–54.
[13] Shen SF, Bian YY, Zhao Y. Energy-efficient CO_2 capture using potassium prolinate/ethanol solution as a phase-changing absorbent. Int J Greenh Gas Con 2017;56:1–11.
[14] Li XQ, Ding YD, Guo LH, Liao Q, Zhu X, Wang H. Non-aqueous energy-efficient absorbents for CO_2 capture based on porous silica nanospheres impregnated with amine. Energ 2019;171:109–19.
[15] Kim H, Rajamanickam R, Park JW. Carbonation and decarbonation of non-aqueous solutions with different compositions of ethylene glycol and various amidines. Int J Greenh Gas Con 2017;59:91–8.
[16] Liu F, Jing GH, Zhou XB, Lv BH, Zhou ZM. Performance and mechanisms of triethylene tetramine (TETA) and 2-amino-2-methyl-1-propanol (AMP) in aqueous and nonaqueous solutions for CO_2 capture. ACS Sustain Chem Eng 2018;6:1352–61.
[17] Guo H, Li CX, Shi XQ, Li H, Shen SF. Nonaqueous amine-based absorbents for energy efficient CO_2 capture. Appl Energ 2019;239:725–34.
[18] Xiao M, Liu HL, Gao HX, Olson W, Liang ZW. CO_2 capture with hybrid absorbents of low viscosity imidazolium-based ionic liquids and amine. Appl Energ 2019;235:311–9.
[19] Bougie F, Pokras D, Fan X. Novel non-aqueous MEA solutions for CO_2 capture. In. J. Greenh. Gas Con. 2019;86:34–42.
[20] Barbarossa V, Barzagli F, Mani F, Lai S, Stoppioni P, Vanga G. Efficient CO_2 capture by non-aqueous 2-amino-2-methyl-1-propanol (AMP) and low temperature solvent regeneration. RSC Adv 2013;3:12349–55.
[21] Yang DZ, Lv M, Chen J. Efficient non-aqueous solvent formed by 2-piperidineethanol and ethylene glycol for CO_2 absorption. Chem. Commun. 2019;55:12483–6.
[22] Nwaoha C, Saiwan C, Supap T, Idem R, Tontiwachwuthikul P, Rongwong W, et al. Carbon dioxide (CO_2) capture performance of aqueous tri-solvent blends containing 2-amino-2-methyl-1-propanol (AMP) and methyldiethanolamine (MDEA) promoted by diethylenetriamine (DETA). Int J Greenh Gas Con 2016;53:292–304.
[23] Tan LS, Shariff AM, Lau KK, Bustam MA. Impact of high pressure on high concentration carbon dioxide capture from natural gas by monoethanolamine/ N-methyl-2-pyrrolidone solvent in absorption packed column. Int J Greenh Gas Con 2015;34:25–30.
[24] Kim H, Hwang SJ, Lee KS. Novel shortcut estimation method for regeneration energy of amine solvents in an absorption-based carbon capture process. Environ Sci Technol 2015;49:1478–85.

[25] Liu F, Fang MX, Dong WF, Wang T, Xia ZX, Wang QH, et al. Carbon dioxide absorption in aqueous alkanolamine blends for biphasic solvents screening and evaluation. Appl Energ 2019;233:468–77.
[26] Nwaoha C, Saiwan C, Supap T, Idem R, Tontiwachwuthikul P, Al-Marri MJ, et al. Regeneration energy analysis of aqueous tri–solvent blends containing 2-amino-2-methyl-1-propanol (AMP), methyldiethanolamine (MDEA) and diethylenetriamine (DETA) for carbon dioxide (CO_2) capture. Energ Procedia 2017;114:2039–46.
[27] Wu KX, Zhou XB, Wu XM, Lv BH, Jing GH, Zhou ZM. Understanding the corrosion behavior of carbon steel in amino-functionalized ionic liquids for CO_2 capture assisted by weight loss and electrochemical techniques. Int J Greenh Gas Con 2019;83:216–27.
[28] Zhao WB, Zhao Q, Zhang Z, Liu JJ, Chen R, Chen Y, et al. Liquid-solid phase-change absorption of acidic gas by polyamine in nonaqueous organic solvent. Fuel 2017;209:69–75.
[29] Svensson H, Velasco VZ, Hulteberg C, Karlsson HT. Heat of absorption of carbon dioxide in mixtures of 2-amino-2-methyl-1-propanol and organic solvents. Int J Greenh Gas Con 2014;30:1–8.
[30] Kawase M, Ido A, Morinaga M. Development of $SiO_2/TiO_2/Al_2O_3$-based/TiO_2 coating for preventing sulfide corrosion in thermal power plant boilers. Appl Therm Eng 2019;153:242–9.
[31] Campbell KLS, Zhao YC, Hall JJ, Williams DR. The effect of CO_2-loaded amine solvents on the corrosion of a carbon steel stripper. Int J Greenh Gas Con 2016;47:376–85.
[32] Lv BH, Jing GH, Qian YH, Zhou ZM. An efficient absorbent of amine-based amino acid-functionalized ionic liquids for CO_2 capture: high capacity and regeneration ability. Chem Eng J 2016;289:212–8.
[33] Kortunov PV, Baugh LS, Siskin M, Calabro DC. In situ nuclear magnetic resonance mechanistic studies of carbon dioxide reactions with liquid amines in mixed base systems: The interplay of lewis and bronsted basicities. Energ Fuel 2015;29:5967–89.
[34] Lv BH, Guo BS, Zhou ZM, Jing GH. Mechanisms of CO_2 capture into monoethanolamine solution with different CO_2 loading during the absorption/desorption processes. Environ Sci Technol 2015;49:10728–35.
[35] Svensson H, Edfeldt J, Velasco VZ, Hulteberg C, Karlsson HT. Solubility of carbon dioxide in mixtures of 2-amino-2-methyl-1-propanol and organic solvents. Int J Greenh Gas Con 2016, 2014,;27(8):247–54.
[36] Lin PH, Wong DSH. Carbon dioxide capture and regeneration with amine/alcohol/water blends. Int J Greenh Gas Con 2014;26:69–75.
[37] Nwaoha C, Idem R, Supap T, Saiwan C, Tontiwachwuthikul P, Rongwong W, et al. Heat duty, heat of absorption, sensible heat and heat of vaporization of 2-Amino-2-Methyl-1-Propanol (AMP), Piperazine (PZ) and Monoethanolamine (MEA) tri-solvent blend for carbon dioxide (CO_2) capture. Chen Eng Sci 2017;170:26–35.
[38] Gao JB, Cao LD, Dong HF, Zhang XP, Zhang SJ. Ionic liquids tailored amine aqueous solution for pre-combustion CO_2 capture: role of imidazolium-based ionic liquids. Appl Energ 2015;154:771–80.